Synthesis and bio-functionalization of multifunctional magnetic Fe$_3$O$_4$@Y$_2$O$_3$:Eu nanocomposites

Zhi Ya Ma[a], **Dosi Dosev**[a], **Mikaela Nichkova**[b], **Shirley J. Gee**[b], **Bruce D. Hammock**[b], and **Ian M. Kennedy**[*,a]

[a]Department of Mechanical and Aeronautical Engineering, University of California Davis, One Shields Avenue, Davis, CA, 95616, USA.

[b]Department of Entomology, University of California Davis, One Shields Avenue, Davis, CA, 95616, USA

Abstract

A facile homogenous precipitation method has been developed for the synthesis of multifunctional, magnetic, luminescent nanocomposites with Fe$_3$O$_4$ nanoparticles as the core and europium-doped yttrium oxide (Y$_2$O$_3$:Eu) as the shell. The nanocomposites showed both super-paramagnetic behavior and unique europium fluorescence properties with high emission intensity. Their surface has been modified with a bifunctional ligand, *p*-aminobenzoic acid (PABA), and further biofunctionalized with biotin; the nanocomposites showed specific targeting for avidin-coupled polystyrene beads.

1. Introduction

Multifunctional nanocomposites that possess desirable properties in a single entity have attracted broad interest in recent years. For instance, nanocomposites with both fluorescent and magnetic properties can be used in a wide range of applications in biological systems, such as bioimaging, diagnostic, and therapeutics. [1-5] They can serve as luminescent markers; they can also be controlled by an external magnetic field. Most of the magnetic fluorescent nanocomposites are core–shell structures with the great majority of emitters being either quantum dots (QDs) or organic dyes.

Several efforts have been directed toward the development of magnetic fluorescent nanocomposites—the preparation methods can be grouped into four classes: (1) a magnetic core coated with silica,[6,7] polymer[8] or lipid[9] containing fluorescent components; (2) a magnetic core covalently bound to a fluorophore *via* a spacer;[10,11] (3) a magnetic core directly coated with a fluorescent shell;[12-14] (4) magnetic nanoparticles and QDs encapsulated in a polymer or silica matrix.[15,16] Although organic dyes are widely applied in the life sciences, they have some problems such as broad spectral features, short lifetimes, photo-bleaching, decomposition and potential toxicity to cells. Compared with organic dyes, QDs display high photostability, size-dependent emissions, high quantum yields and narrow emission band-widths. However, QDs have not achieved universal acceptance because of their inherent toxicity, chemical instability and difficult surface conjugation chemistry.

In addition to organic dyes and QDs, lanthanide-doped nanoparticles are gaining popularity and have been recognized as a promising new class of fluorescent biological label due to the

Department of Mechanical and Aeronautical Engineering, University of California Davis, One Shields Avenue, Davis, CA, 95616, USA. imkennedy@ucdavis.edu; Fax: +1 530 210 8220; Tel: +1 530 752 2796.

unique luminescence properties, such as large Stokes shifts, narrow line-width emission bands, high quantum yields, long lifetimes and superior photostability.[17] In contrast to semi-conductor QDs, the emission wavelength of the lanthanide nanoparticles is independent of particle size and hence mono-dispersity is less crucial, leading to lower synthesis costs. Furthermore, surface modification does not significantly affect their optical properties, because their luminescence arises as a result of electronic transitions of the lanthanide ion. In particular, they also offer excellent chemical stability, high quantum yield and probably low toxicity.

At present there is only a limited number of reports on the application of lanthanide-doped nanoparticles in biology.[18,19] The examples include lanthanide chelate-doped polystyrene and silica nanoparticles,[20,21] lanthanide fluorides[22] and lanthanide oxides.[23–26] To apply the lanthanide-doped nanoparticles as biolabels, many schemes have been developed for the functionalization of the surfaces of the nanoparticles for subsequent bioconjugation. The functionalization methods can be divided into three groups: (1) direct silanization using a variety of functionalized alkoxysilanes or *via* silica coating;[24,27] (2) physical adsorption with protein or polymer *via* hydrophobic or electrostatic forces;[23,25] (3) coordination using bifunctional ligands.[28,29] Among these methods, silanization is most common. However, silanization requires a tedious procedure for coating the particles with silica which is hard to reproduce and often leads to the aggregation of particles. Physical adsorption is easy to perform but the non-specific adsorption and the random immobilization of biomolecules (for example, antibodies) are unavoidable. Coordination to the surface of the particles with bifunctional ligands has been demonstrated to be an efficient way to modify the nanoparticle surface. These ligands usually contain two functional groups with one group attached to the surface of the nanoparticles—the other one can be used for the conjugation of biomolecules. For example, Diamente *et al.*[28] have modified Ln^{3+}-doped LaF_3 nanoparticles with amino groups by coordinating the surface through the phosphate end of a bifunctional ligand, 2-aminoethyl phosphate, for avidin bioconjugation. Meiser *et al.*[29] functionalized $LaPO_4$:Ce/Tb nanoparticles with streptavidin by using a bifunctional ligand 6-aminohexanoic acid (AHA) for biotin–streptavidin binding studies.

To the best of our knowledge, there are few reports on the combination of magnetic properties with lanthanide nano-phosphors. Lu *et al.*[30] deposited a shell of up-converting phosphor (ytterbium and erbium co-doped sodium yttrium fluoride) on an iron oxide core. Our group has recently developed a flame spray pyrolysis method for the synthesis of magnetic luminescent core–shell particles consisting of magnetic cores and luminescent shells of europium-doped gadolinium oxide (Gd_2O_3:Eu) and applied them in immunoassay and DNA detection.[31–34] The spray pyrolysis method is a cost-effective, high throughput and versatile synthesis method for the synthesis of magnetic luminescent particles. However, because it needs some special apparatus, it might not be easily realized in a common laboratory. Furthermore, the resulting particles have a wide size distribution and irregular shape, which might hinder their applications in some biological fields with requirements for more uniform size particles.

In this paper, we report the development of a facile homogenous precipitation method for the preparation of multifunctional magnetic fluorescent nanocomposites with Fe_3O_4 nanoparticles as the core and Eu^{3+}-doped yttrium oxide (Y_2O_3:Eu) as the shell. Then we used a bifunctional ligand, *p*-aminobenzoic acid (PABA), to introduce the amino groups to the surfaces of the nanocomposites. The nanoparticles were biofunctionalized with biotin. Finally, to test the ability of these biotin-functionalized nanocomposites to be applied in biomedicine, avidin-coupled polystyrene beads were used as a model cellular mimic for demonstrating specific targeting and cell sorting.

2. Experimental section

2.1 Reagents and materials

Ferric chloride hexahydrate ($FeCl_3 \cdot 6H_2O$), ferrous chloride tetrahydrate ($FeCl_2 \cdot 4H_2O$), ammonium hydroxide (28–30% NH_3), poly(ethylene glycol) (PEG, MW 10 000), urea, *p*-aminobenzoic acid (PABA), fluorescein isothiocyanate (FITC), yttrium nitrate hexahydrate (Y$(NO_3)_3 \cdot 6H_2O$, 99.99%), europium nitrate pentahydrate ($Eu(NO_3)_3 \cdot 5H_2O$, 99.95%), bovine serum albumin (BSA) and dimethyl sulfoxide (DMSO) were purchased from Sigma-Aldrich and used as received. *EZ*-Link sulfo-NHS-biotin was from Pierce (Rockford, IL). SuperAvidin-coated beads (mean diameter of $15.7 \pm 0.4\,\mu m$) and Dragon green (excitation 480 nm, emission 520 nm) polystyrene beads (mean diameter of $7.32 \pm 0.5\,\mu m$) were purchased from Bangs Laboratories, Inc. (Fishers, IN). PBS is phosphate buffer saline (pH 7.4). PBST is PBS containing 0.05% Tween 20.

2.2 Synthesis of PEG-coated magnetic Fe_3O_4 nanoparticles

PEG-coated magnetic Fe_3O_4 nanoparticles were prepared by the co-precipitation method as described before with modifications. [35] Briefly, 2.36 g of $FeCl_3 \cdot 6H_2O$ and 0.86 g of $FeCl_2 \cdot 4H_2O$ (2 : 1 molar ratio) were added to 40 mL of deionized water and stirred under nitrogen. A total of 5 mL of ammonium hydroxide was added quickly at 90 °C under rapid mechanical stirring. Due to the large surface area-to-volume ratios and magnetic dipole–dipole attraction between magnetic nanoparticles, the magnetic nanoparticles aggregated readily. To get very stable and highly water soluble magnetic nanoparticles, PEG was used as a coating polymer during the co-precipitation process. It is known that PEG is a hydrophilic and biocompatible polymer and its very high surface mobility leads to high steric exclusion. Therefore, 5 mL of PEG aqueous solution were added dropwise, and the suspension was kept at 90 °C for 1 h. The resultant black magnetite nanoparticles were separated magnetically, and washed with de-ionized (DI) water and ethanol several times, and stored in ethanol.

2.3 Synthesis of magnetic Fe_3O_4@Y_2O_3:Eu nanocomposites

A Eu^{3+}-doped yttrium oxide (Y_2O_3:Eu) fluorescent shell was coated on the magnetic Fe_3O_4 nanoparticles using a homogenous precipitation method (Scheme 1). In a typical procedure, 10 mg of PEG-coated magnetic Fe_3O_4 nanoparticles were dispersed in 50 mL of DI water containing 1.8 M urea and 5 mM $Ln(NO_3)_3$ (Ln = Y, Eu; Eu^{3+} doping concentration was 5 at %). The mixture was sonicated for 20 min and then heated to 90 °C under vigorous mechanical stirring. After 4 h, the resultant precursor was separated with a magnet, thoroughly washed with ethanol and water several times, and further dried at 100 °C overnight. Finally, the precursor particles were calcinated at 700 °C for 2 h for complete conversion to the oxide. The resulting magnetic nanocomposites were magnetic Fe_3O_4@Y_2O_3:Eu nanocomposites.

2.4 Bio-functionalization of magnetic Fe_3O_4@Y_2O_3:Eu nanocomposites

10 mg of magnetic Fe_3O_4@Y_2O_3:Eu nanocomposites were dispersed in 10 mL of ethanol solution containing 0.2 g of PABA. The solution was stirred at room temperature overnight. After being separated magnetically and washed with ethanol several times, the nanocomposites were dried in the oven.

Fe_3O_4@Y_2O_3:Eu nanocomposites were biotinylated as follows: 2mg of nanocomposites were suspended in 1mL of PBS; sulfo-NHS-biotin (0.4 mL of 6 mg mL^{-1}) was added and incubated for 1.5 h in a rotating mill at rt; after the reaction was completed the nanocomposites were separated on the magnet and washed three times with PBS.

2.5 Application of biotinylated Fe$_3$O$_4$@Y$_2$O$_3$:Eu nanocomposites to magnetic extraction of avidin-coated beads

The beads were washed according to manufacturer's instructions by centrifugation (1200*g* for 15 min) and blocked with 0.5% BSA–PBS for 1 h in a rotating mill. After centrifugation, they were re-suspended in 0.2% BSA–PBST, added to the biotinylated Fe$_3$O$_4$@Y$_2$O$_3$:Eu nanocomposites. 50 µg of magnetic nano-composites, ~0.4 × 10^6 SuperAvidin-coated beads and ~0.4 × 10^6 Dragon green beads were used per reaction (total volume 500 µL). The avidin–biotin interaction took place over 30 min, in a rotating mill at rt. Then, the avidin-coated beads bound to the biotinylated magnetic fluorescent nanocomposites were extracted from the solution using a magnet and washed three times with PBST and once with water. The extracted nanoparticles were re-suspended in 100 µL of water.

2.6 Characterization of the nanocomposites

The size and the morphology of the particles were examined by using a Philips CM-12 transmission electron microscope (TEM). Samples were prepared by placing a drop of a dilute ethanol dispersion of particles on the surface of a copper grid. The average size of the Fe$_3$O$_4$ nanoparticles and nanocomposites was determined by averaging the sizes of 100 particles measured in different TEM images. The hydrodynamic diameters of PABA-modified magnetic nanocomposites in water were measured by dynamic light scattering (DLS). The surface functionalization of nanocomposites with PABA was confirmed by Fourier transform infrared spectroscopy (FTIR) using KBr pellets.

The structure of the particles was characterized using X-ray powder diffraction (X'Pert Philips Materials Research Diffractomer) using a Cu Kα radiation source. The magnetic properties were measured on a vibrating magnetometer at 300 K. Fluorescence spectra measurements were performed on a Spectramax M2 cuvette/microplate reader. Confocal laser-scanning microscopy was performed using an Olympus FV1000. The quantum yields of the aqueous solutions of magnetic Y$_2$O$_3$:Eu nanocomposites with and without PABA modification were measured by comparing the emissions of the solution to the emission of a solution of Rhodamin 6G of identical optical density at the excitation wavelength.

3. Results and discussion

Fig. 1A shows a TEM image of PEG-coated Fe$_3$O$_4$ nanoparticles. It can be seen that the particles were almost spherical with average diameters of about 15 nm. Although the particles should remain discrete entities due to the high steric exclusion properties of PEG hydrophilic chains located at the surface of the nanoparticles, there was still some apparent aggregation in the TEM images, which might be because of the cross-linkage of the PEG chains due to hydrogen bonding; TEM sample preparation and drying can also lead to apparent aggregation.

As well as size determination established by TEM, the hydrodynamic size of the nanocomposites in aqueous solution was measured using DLS. Compared with the 'dry' size of 80 nm measured by TEM, Fig. 1D shows that the PABA-modified magnetic nanocomposites have an average hydrodynamic diameter of about 85 nm. The larger diameter observed from DLS analysis included not only the nanocomposites core, which is measurable using TEM, but also the hydrodynamic diameter from the PABA coating and the hydrated layer. The presence of active amino groups on the PABA-modified nanocomposites was determined by the assessment of FTIR spectra as well. Spectra of PABA-modified nanocomposites showed characteristic peaks at 3500 cm^{-1} and 1623 cm^{-1} (amino groups) (data not shown), indicating that the modification with PABA was successful.

To coat the magnetic Fe_3O_4 nanoparticles with a fluorescent Y_2O_3:Eu shell, a homogenous precipitation method was applied first to cover the Fe_3O_4 surface with a shell of yttrium basic carbonate by mixing a suspension of the PEG-coated Fe_3O_4 nanoparticles with urea and Ln $(NO_3)_3$ aqueous solution and heating at 90 °C for 4 h. Then the yttrium basic carbonate shell was converted into yttrium oxide by calcination at 700 °C for 2 h.

The homogenous precipitation method has been demonstrated to be efficient for the preparation of Y_2O_3 particles with narrow size distribution. The basis for the homogenous precipitation is that when a certain type of organic compound, such as urea, is dissolved in a solution containing metal cations, the generated anions (*e.g.*, OH^-, CO_3^{2-}) will form precipitation nuclei with metal cations above a critical supersaturation. The generated anions are consumed by the growth of nuclei and no new nuclei form. This leads to a controlled separation of nucleation and growth of precipitates. Thus monodispersed particles are produced.[36] According to Sohn *et al.*,[37] the reaction mechanism of the formation of yttria precursor particles through homogenous precipitation includes two steps: urea decomposition and yttrium precipitation. Urea decomposition generates OH^- and CO_3^{2-}. Then these anions can precipitate with yttrium ions to form yttrium basic carbonate ($Y(OH)CO_3$). The overall reaction is:

$$Y^{3+}+(NH_2)_2CO + 4H_2O = Y(OH)CO_3 \cdot H_2O + 2NH_4^+ + H^+ \tag{1}$$
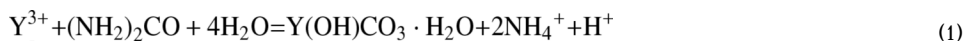
Fig. 1B shows the TEM image of Fe_3O_4 coated with yttrium basic carbonate, indicating that the particles are well dispersed, nearly spherical with a relatively narrow size distribution. The average size is about 100 nm. Fig. 1C presents the TEM image of $Fe_3O_4@Y_2O_3$:Eu nanocomposites. After calcination, the particles are still well dispersed and the spherical shape remains. It can be noted that a small change in size and a loss in weight were also observed. The average size of the particles becomes about 80 nm.

In order to investigate the structure and composition of the hybrid nanoparticles, XRD was employed to analyze the samples. Fig. 2 shows the X-ray diffraction pattern of magnetic nanocomposites after calcination at 700 °C. It shows that magnetic nanocomposites exhibit the characteristic diffraction peaks of Y_2O_3 (marked with ■) with cubic structure and additional peaks that coincide with the peaks of either cubic spinel Fe_3O_4 or γ-Fe_2O_3 (marked with ●). Our experimental data cannot clearly distinguish between these two types of iron oxide because they have very similar magnetic properties. Because both of them are magnetic, unambiguous identification is not essential in the present study.

The magnetic hysteresis loop of the magnetic $Fe_3O_4@Y_2O_3$:Eu nanocomposites taken at room temperature is shown in Fig. 3. The samples display super-paramagnetic properties (zero coercivity and resonance), which is crucial for their application in biomedicine and biotechnology because it prevents magnetic particle aggregation and enables them to re-disperse rapidly when the magnetic field is removed. The saturation magnetization value of $Fe_3O_4@Y_2O_3$:Eu nanocomposites is 4.3 emu g^{-1}. Fig. 4 illustrates the magnetic separation of an aqueous dispersion of the magnetic $Fe_3O_4@Y_2O_3$:Eu nanocomposites. When an external magnetic field is applied beside the glass vial, the nanocomposites can be directed to the magnet very quickly. These magnetic properties will allow the nanocomposites to be used in biomedical applications since they undergo strong magnetization, allowing efficient magnetic delivery, concentration and separation.

Fig. 5 shows the luminescent emission spectra of the synthesized $Fe_3O_4@Y_2O_3$:Eu nanocomposites which is typical of the shell material Y_2O_3:Eu. Under excitation at 260 nm, the particles with a Y_2O_3:Eu shell emitted red luminescence with a narrow peak centered at 610 nm, which can be assigned to the transition from the $^5D_0$ excited state to the $^7F_2$ state. The

quantum yields of the aqueous solutions of magnetic Y_2O_3:Eu nanocomposites with and without PABA modification were found to be 14% and 10.2%, respectively. The quantum yields are lower than for the bulk materials, which might be because the nanoscale sized nanocomposites have a large surface-to-volume ratio and thus will be much more strongly influenced by properties of the particle surface than is the case for bulk materials. Furthermore, in aqueous solution, the adsorbed water on the surface of the nanocomposites will result in extensive quenching. The reason for the decrease of quantum yield after surface modification with PABA is not clear. It must have some relation to the PABA which coordinates to the yttrium or europium cations on the surface of the nanocomposites.

To test the ability of synthesized $Fe_3O_4@Y_2O_3$:Eu nanocomposites to be used in bioimaging and bio-labeling, the surfaces of the nanocomposites were functionalized with biotin for binding with avidin-coupled polystyrene beads. As part of this procedure, the primary requirement was to first obtain stable aqueous colloids of the nanocomposites. This was achieved by dispersing the magnetic $Fe_3O_4@Y_2O_3$:Eu nanocomposites in an ethanol solution containing the bifunctional ligand, PABA. It has been demonstrated that the molecules with carboxyl groups can efficiently functionalize the iron oxide surface of the nanoparticles by coordination to surface metal ions with carboxyl groups.[38,39] We assumed that this modification should also be applicable to our particles with yttrium oxide surfaces. The carboxyl group of PABA should coordinate with the yttrium or europium cations on the surface of the nanocomposites to form a robust coating, while amino groups extend into the aqueous solution, conferring upon the particles a high degree of water dispersibility with the capacity for further linkage of biomolecules through well-developed bioconjugation chemistry. We found that the water dispersibility of the nanocomposites increased greatly after surface modification with PABA. The nanocomposites with PABA modification can be suspended in water (1 mg mL^{-1}) for 2 days at room temperature without obvious sedimentation while the nanocomposites without modification can only be suspended in water for 2 h. The successful modification of nanocomposites with amino groups on the surface was evaluated by their covalent coupling to FITC. The detailed procedure was as follows: magnetic nanocomposites (1 mg) were suspended in 1 mL of carbonate–bicarbonate buffer (pH 8.6) and 100 μL of 25mg mL^{-1} FITC solution in anhydrous dimethyl formamide was added. The coupling reaction took place for 1 h at room temperature in a rotating mill. The excess dye was removed by three cycles of centrifugation and washing of the nanocomposites with buffer. The FITC-conjugated nanocomposites were suspended in carbonate–bicarbonate buffer, and the fluorescence intensity was measured on a microplate reader (excitation at 490 nm). The characteristic emission peak of FITC at 520 nm (data not shown) indicated the presence of amino groups on the surface of the nanocomposites. The amino groups from the surface of the functionalized nanoparticles were easily biotinylated using sulfo-NHS-biotin.

In order to demonstrate the applicability of the magnetic fluorescent nanoparticles in cell separation bioassays, we chose to use avidin-coated polystyrene beads (mean diameter of 15.7 ± 0.4 μm) as a mimic of cells bearing a specific surface protein. The presence of "non-specific cells" was simulated by the presence of Dragon green polystyrene beads (mean diameter of 7.32 ± 0.5 μm) that were used as a negative control. Specific targeting of magnetic $Fe_3O_4@Y_2O_3$:Eu nanocomposites was examined by incubation of the mixed cellular mimic models (polystyrene beads). As shown in Fig. 6, confocal laser-scanning microscope images confirmed the specific targeting of nanocomposites to the avidin–polystyrene beads. On the other hand, the small fluorescent Dragon green polystyrene beads without avidin on the surface were not targeted, indicating the absence of nonspecific binding. Due to the fact that the nanocomposites have biotin ligands on their surface, biotin binding to the avidin– polystyrene beads with a large excess of nanoparticles should approach that of an irreversible reaction, given that the biotin–avidin has an affinity constant in the range of 10^{-15} M.

4. Conclusion

Multifunctional magnetic $Fe_3O_4@Y_2O_3$:Eu nanocomposites have been successfully prepared by a facile homogenous precipitation method. By surface modification with PABA and subsequent bio-functionalization with biotin, the nanocomposites showed high water solubility and specific targeting to avidin–polystyrene beads. With the advantage of high magnetic responsiveness, unique luminescence properties, high water solubility, and easy coupling of other biomolecules through the same protocol as biotin, we envision that our nanocomposites could be used in a number of biomedical applications, such as targeting, cell separation and bioimaging.

Acknowledgments

References

1. Corr SA, O'Byrne A, Gun'ko YK, Ghosh S, Brougham DF, Mitchell S, Volkov Y, Prina-Mello A. Chem. Commun 2006:4474–4476.

2. Corr SA, Rakovich YP, Gun'ko YK. Nanoscale Res. Lett 2008;3:87–104.

3. Quarta A, Di Corato R, Manna L, Ragusa A, Pellegrino T. IEEE Trans. Nanobiosci 2007;6:298–308.

4. Veiseh O, Sun C, Gunn J, Kohler N, Gabikian P, Lee D, Bhattarai N, Ellenbogen R, Sze R, Hallahan A, Olson J, Zhang MQ. Nano Lett 2005;5:1003–1008. [PubMed: 15943433]

5. Yoon TJ, Kim JS, Kim BG, Yu KN, Cho MH, Lee JK. Angew. Chem., Int. Ed 2005;44:1068–1071.

6. Lu Y, Yin YD, Mayers BT, Xia YN. Nano Lett 2002;2:183–186.

7. Yoon TJ, Yu KN, Kim E, Kim JS, Kim BG, Yun SH, Sohn BH, Cho MH, Lee JK, Park SB. Small 2006;2:209–215. [PubMed: 17193022]

8. Hong X, Li J, Wang MJ, Xu JJ, Guo W, Li JH, Bai YB, Li TJ. Chem. Mater 2004;16:4022–4027.

9. Becker C, Hodenius M, Blendinger G, Sechi A, Hieronymus T, Muller-Schulte D, Schmitz-Rode T, Zenke M. J. Magn. Magn. Mater 2007;311:234–237.

10. Bertorelle F, Wilhelm C, Roger J, Gazeau F, Menager C, Cabuil V. Langmuir 2006;22:5385–5391. [PubMed: 16732667]

11. Huh YM, Jun YW, Song HT, Kim S, Choi JS, Lee JH, Yoon S, Kim KS, Shin JS, Suh JS, Cheon J. J. Am. Chem. Soc 2005;127:12387–12391. [PubMed: 16131220]

12. Du GH, Liu ZL, Lu QH, Xia X, Jia LH, Yao KL, Chu Q, Zhang SM. Nanotechnology 2006;17:2850–2854.

13. Gao JH, Zhang B, Gao Y, Pan Y, Zhang XX, Xu B. J. Am. Chem. Soc 2007;129:11928–11935. [PubMed: 17824703]

14. Gu HW, Zheng RK, Zhang XX, Xu B. J. Am. Chem. Soc 2004;126:5664–5665. [PubMed: 15125648]

15. Tu CF, Yang YH, Gao MY. Nanotechnology 2008;19:8.

16. Yi DK, Selvan ST, Lee SS, Papaefthymiou GC, Kundaliya D, Ying JY. J. Am. Chem. Soc 2005;127:4990–4991. [PubMed: 15810812]

17. Wang LY, Yan RX, Hao ZY, Wang L, Zeng JH, Bao H, Wang X, Peng Q, Li YD. Angew. Chem., Int. Ed 2005;44:6054–6057.

18. Traina CA, Dennes TJ, Schwartz J. Bioconjugate Chem 2008;20:437–439.

19. Dosev D, Nichkova M, Kennedy IM. J. Nanosci. Nanotechnol 2008;8:1052–1067. [PubMed: 18468107]

20. Huhtinen P, Kivela M, Kuronen O, Hagren V, Takalo H, Tenhu H, Lovgren T, Harma H. Anal. Chem 2005;77:2643–2648. [PubMed: 15828805]

21. Zhang H, Xu Y, Yang W, Li QG. Chem. Mater 2007;19:5875–5881.

22. Wang F, Zhang Y, Fan XP, Wang MQ. Nanotechnology 2006;17:1527–1532.

23. Dosev D, Nichkova M, Liu MZ, Guo B, Liu GY, Hammock BD, Kennedy IM. J. Biomed. Opt 2005;10:7.

24. Feng J, Shan GM, Maquieira A, Koivunen ME, Guo B, Hammock BD, Kennedy IM. Anal. Chem 2003;75:5282–5286.

25. Nichkova M, Dosev D, Gee SJ, Hammock BD, Kennedy IM. Anal. Chem 2005;77:6864–6873. [PubMed: 16255584]

26. Nichkova M, Dosev D, Perron R, Gee SJ, Hammock BD, Kennedy IM. Anal. Bioanal. Chem 2006;384:631–637. [PubMed: 16416096]

27. Sivakumar S, Diamente PR, van Veggel FC. Chem.-Eur. J 2006;12:5878–5884.

28. Diamente PR, Burke RD, van Veggel F. Langmuir 2006;22:1782–1788. [PubMed: 16460106]

29. Meiser F, Cortez C, Caruso F. Angew. Chem., Int. Ed 2004;43:5954–5957.

30. Lu HC, Yi GS, Zhao SY, Chen DP, Guo LH, Cheng J. J. Mater. Chem 2004;14:1336–1341.

31. Dosev D, Nichkova M, Dumas RK, Gee SJ, Hammock BD, Liu K, Kennedy IM. Nanotechnology 2007;18:6.

32. Son A, Dhirapong A, Dosev DK, Kennedy IM, Weiss RH, Hristova KR. Anal. Bioanal. Chem 2008;390:1829–1835. [PubMed: 18256809]

33. Son A, Dosev D, Nichkova M, Ma Z, Kennedy IM, Scow KM, Hristova KR. Anal. Biochem 2007;370:186–194. [PubMed: 17869209]

34. Son A, Nichkova M, Dosev D, Kennedy IM, Hristova KR. J. Nanosci. Nanotechnol 2008;8:2463–2467. [PubMed: 18572664]

35. Ma ZY, Guan YP, Liu HZ. J. Magn. Magn. Mater 2006;301:469–477.

36. Sordelet D, Akinc M. J. Colloid Interface Sci 1988;122:47–59.

37. Sohn S, Kwon Y, Kim Y, Kim D. Powder Technol 2004;142:136–153.

38. Ge JP, Hu YX, Biasini M, Dong CL, Guo JH, Beyermann WP, Yin YD. Chem.-Eur. J 2007;13:7153–7161.

39. Sahoo Y, Goodarzi A, Swihart MT, Ohulchanskyy TY, Kaur N, Furlani EP, Prasad PN. J. Phys. Chem. B 2005;109:3879–3885. [PubMed: 16851439]
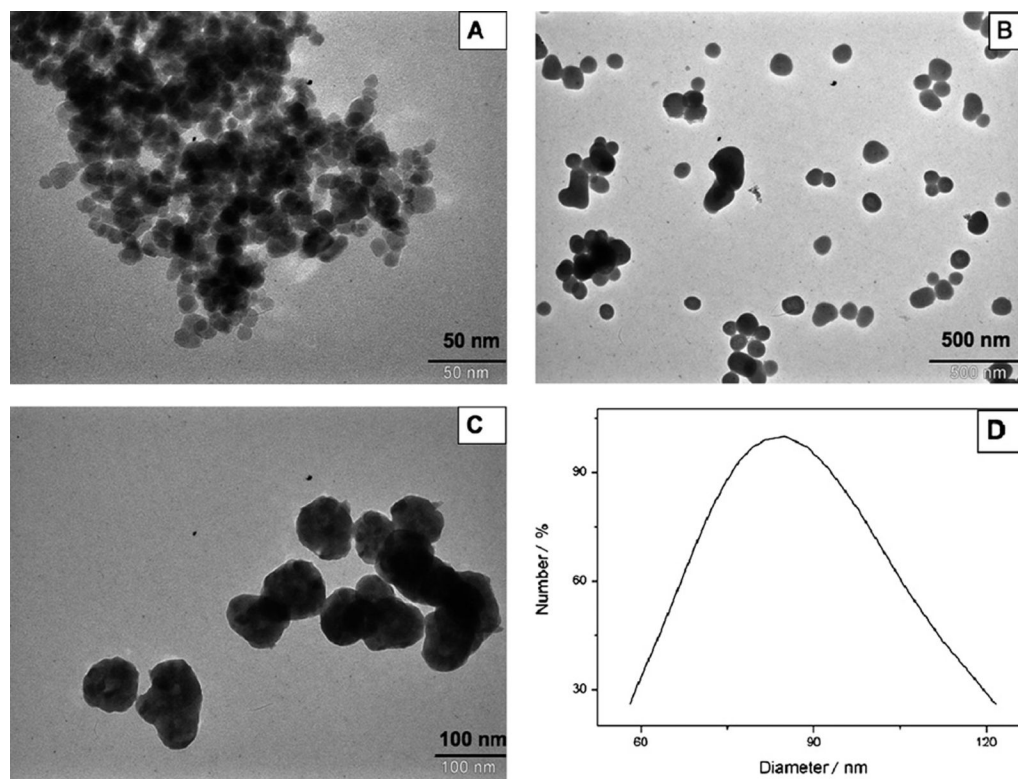
Fig. 1.
TEM images of (A) magnetic Fe_3O_4 nanoparticles, (B) magnetic Fe_3O_4 coated with yttrium precursor, (C) magnetic Fe_3O_4@Y_2O_3:Eu nanocomposites and (D) DLS measurement of particle size distribution.
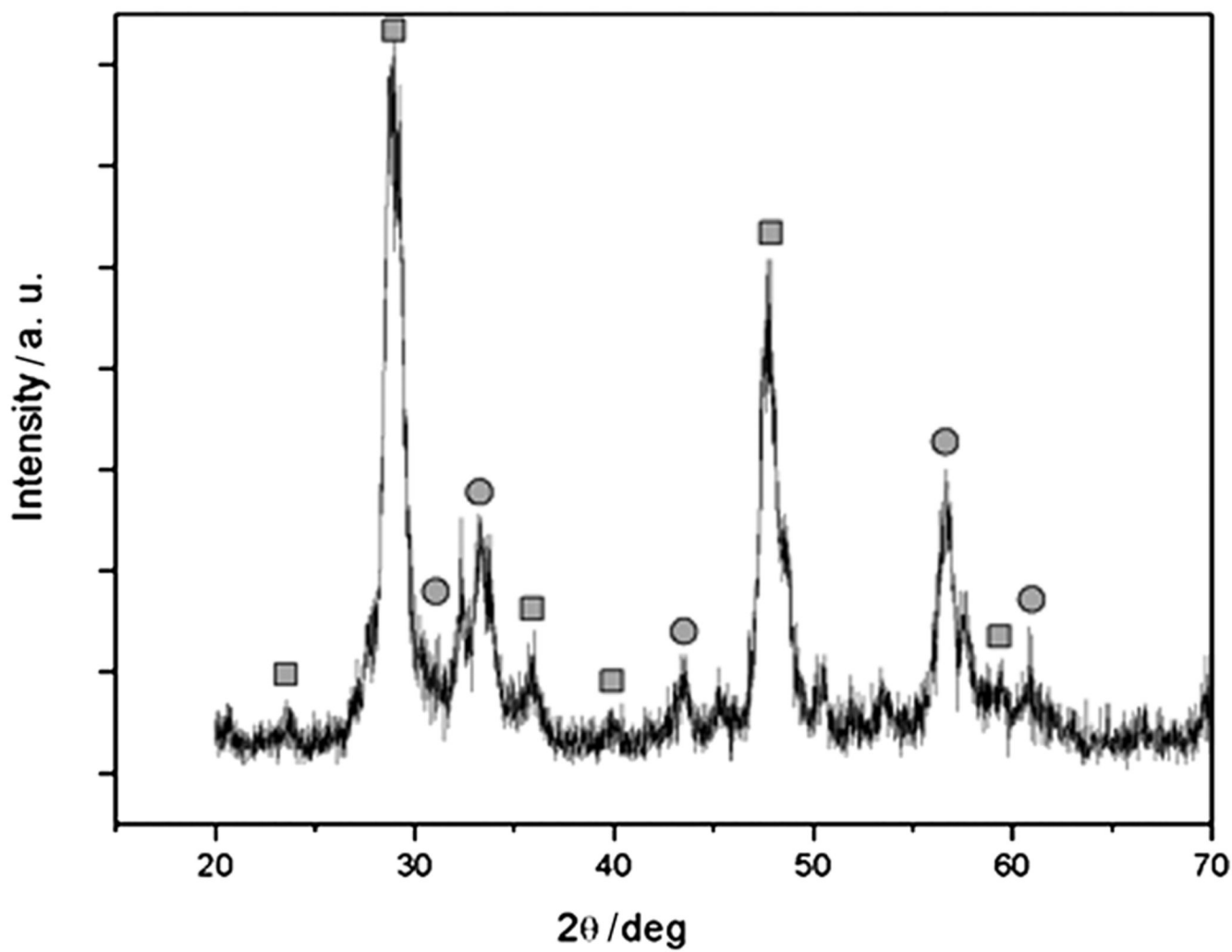
Fig. 2.
XRD patterns of as-prepared magnetic $Fe_3O_4@Y_2O_3$:Eu nanocomposites. The diffraction peaks marked with ■ are indexed to Y_2O_3:Eu, and the peaks marked with ● are indexed to Fe_3O_4.
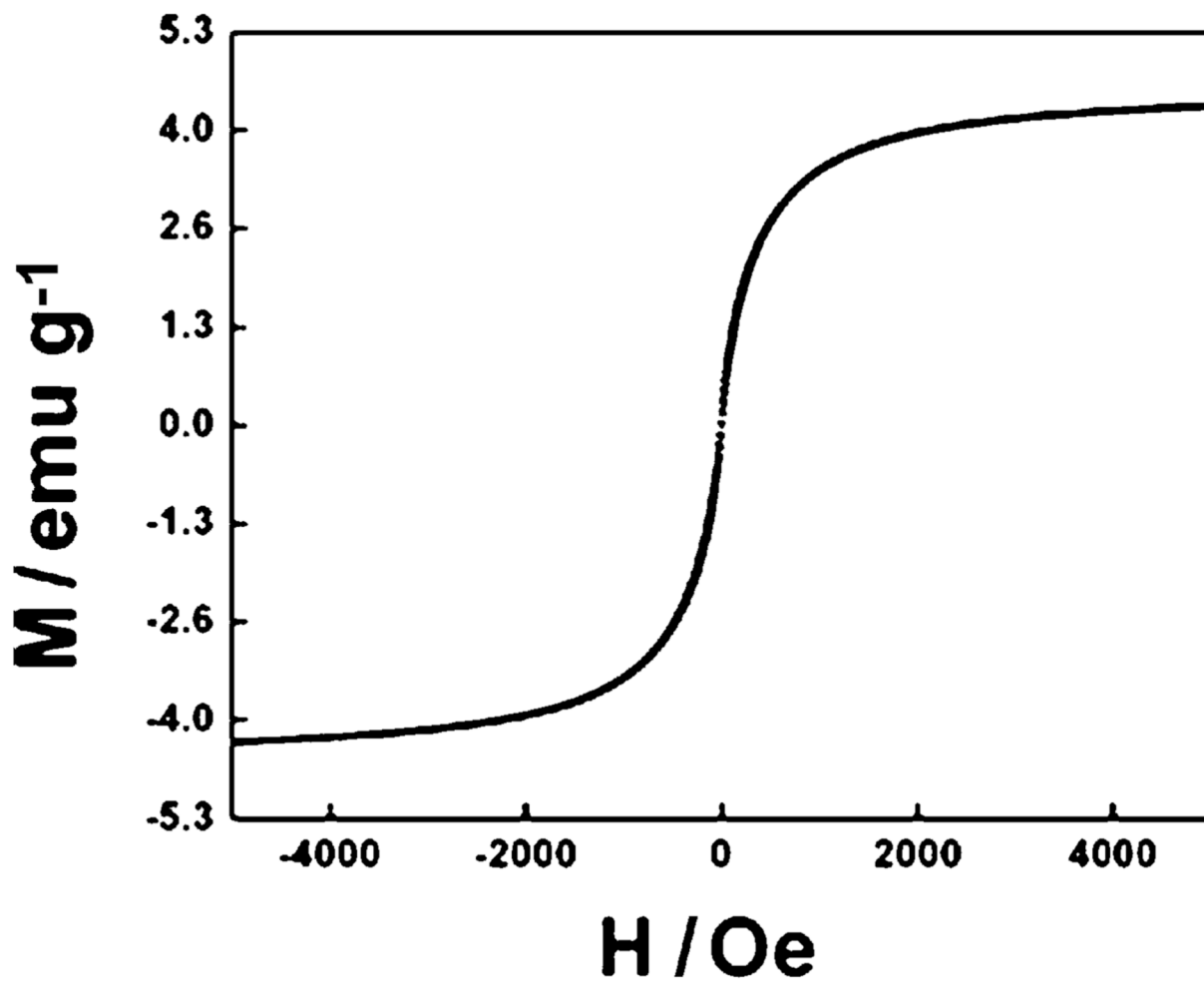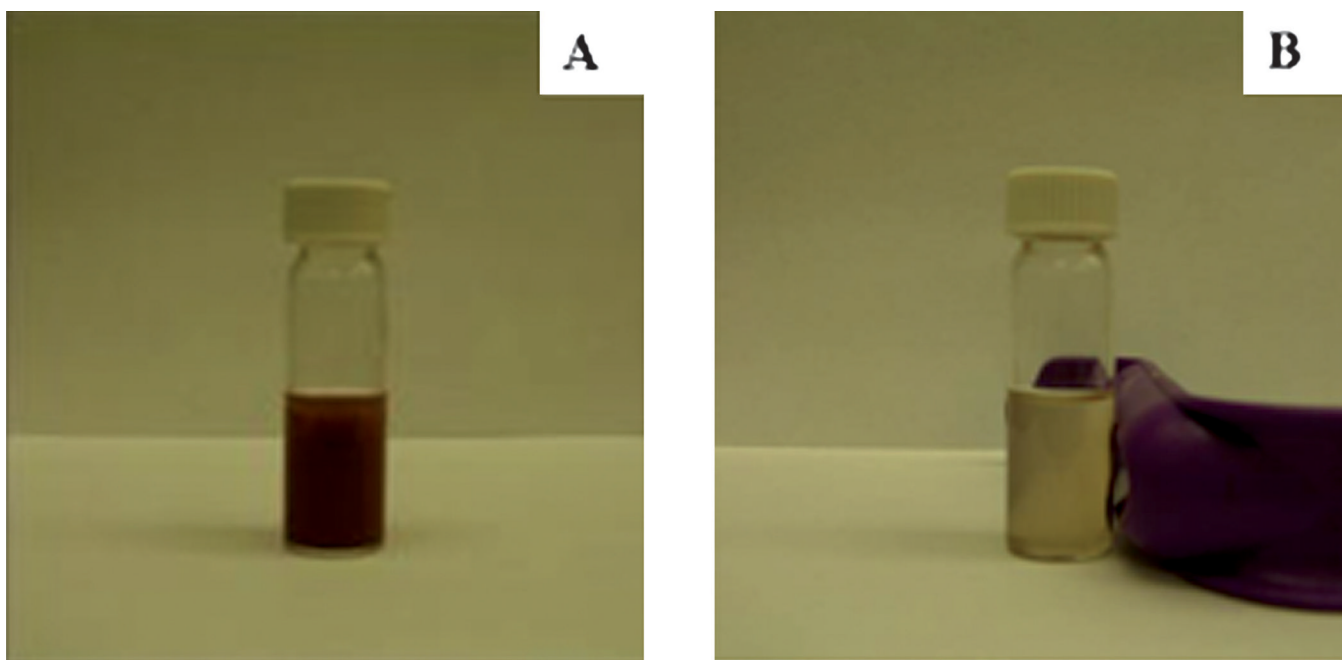
Fig. 3.
Magnetization curve of magnetic $Fe_3O_4@Y_2O_3$:Eu nanocomposites.

Fig. 4.
Photographs of magnetic Fe_3O_4@Y_2O_3:Eu nanocomposites dispersed in aqueous solution (A) without and (B) with external magnetic field.
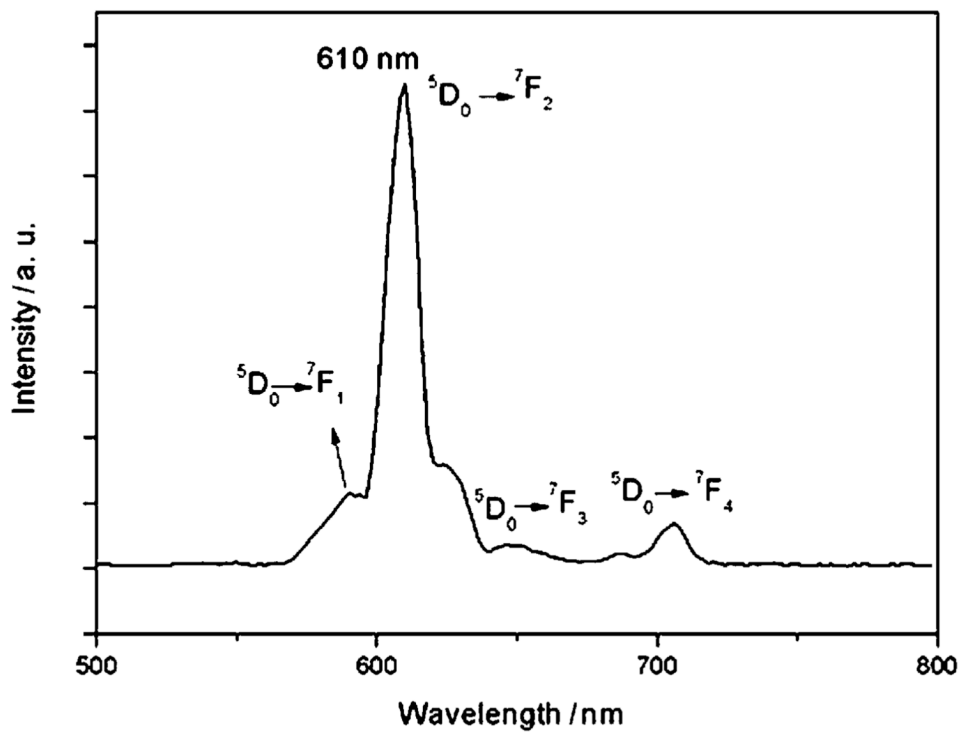
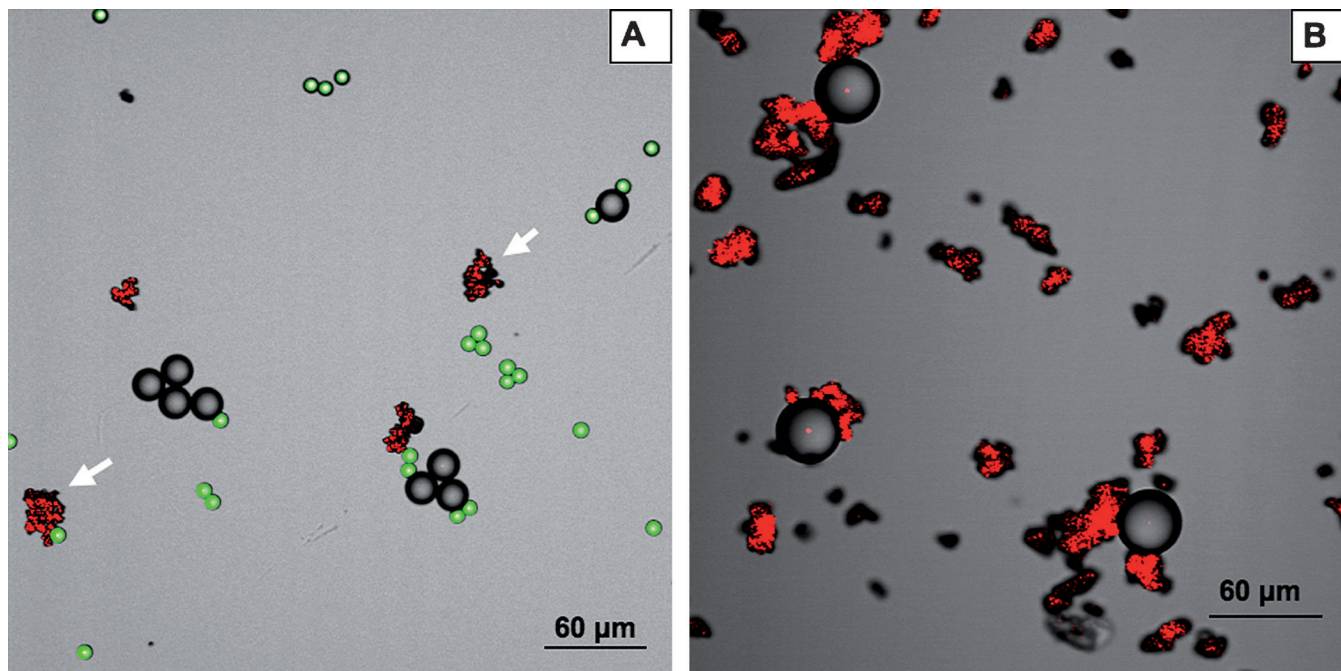**Fig. 5.**
Emission spectra of magnetic Fe_3O_4@Y_2O_3:Eu nanocomposites.

Fig. 6.
Confocal laser-scanning microscopy (CLSM) images of (A) starting mixture of biotinylated magnetic $Fe_3O_4@Y_2O_3$:Eu nanoparticles, avidin-coated polystyrene and Dragon green polystyrene beads. (B) After magnetic extraction: $Fe_3O_4@Y_2O_3$:Eu nanoparticles bearing specifically bound avidin-coated polystyrene beads. The presence of Dragon green polystyrene beads is negligible due to very low non-specific binding of the beads to the surface of the functionalized magnetic nanocomposites. Magnetic $Fe_3O_4@Y_2O_3$:Eu nanocomposites (red), avidin-coupled polystyrene beads (gray) and Dragon green polystyrene beads (green).
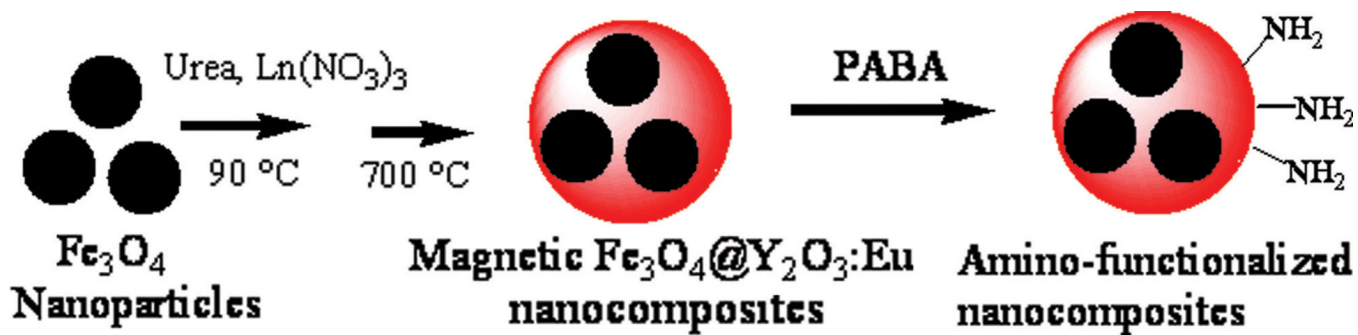
Scheme 1.
Synthetic scheme for the synthesis and surface modification of magnetic $Fe_3O_4@Y_2O_3$:Eu nanocomposites.